A Fast-Converging MPPT Technique for Photovoltaic System Under Fast-Varying Solar Irradiation and Load Resistance

Tey Kok Soon and Saad Mekhilef, *Senior Member, IEEE*

***Abstract*—Under fast-varying solar irradiation and load resistance, a fast-converging maximum power point tracking (MPPT) system is required to ensure the photovoltaic (PV) system response rapidly with minimum power losses. Traditionally, maximum power point (MPP) locus was used to provide such a fast response. However, the algorithm requires extra control loop or intermittent disconnection of the PV module. Hence, this paper proposes a simpler fast-converging MPPT technique, which excludes the extra control loop and intermittent disconnection. In the proposed algorithm, the relationship between the load line and the *I–V* curve is used with trigonometry rule to obtain the fast response. Results of the simulation and experiment using single-ended primary-inductor converter showed that the response of the proposed algorithm is four times faster than the conventional incremental conductance algorithm during the load and solar irradiation variation. Consequently, the proposed algorithm has higher efficiency.**

***Index Terms*—Fast converging, incremental conductance, maximum power point tracking (MPPT), photovoltaic (PV) system, single-ended primary-inductor converter (SEPIC).**

I. Introduction

SOLAR ENERGY is gaining popularity in the field of electricity generation. The advantages of solar power, such as no air pollution, no fuel costs, noiseless, and low maintenance, have boosted the demand on this type of energy as mentioned in [1]–[3]. However, the high expense in acquiring the photovoltaic (PV) module has slowed down the adoption of PV system in electricity generation. Furthermore, the power of PV modules is unstable and strongly dependent on solar irradiation and load. Hence, the maximum power point tracking (MPPT) controller is introduced to ensure the PV system always provide high efficiency despite the variation in solar irradiation and load resistance [6]–[9].

Many MPPT algorithms have been introduced to improve the efficiency of the PV system, including fractional open circuit voltage, fractional short circuit current, fuzzy logic, neural network, hill climbing or perturbation and observation (P&O), and incremental conductance [8]–[21]. Among those algorithms, P&O and incremental conductance are the most popular algorithms. If a dc–dc converter is connected in between the PV module and the load, the switching duty cycle of the dc–dc converter is regulated to ensure the PV system always operates at the maximum power point (MPP) [22]. For P&O, the power of the PV module is determined, and then the duty cycle of the converter is either increased or decreased to achieve the MPP [22]–[26]. Generally, the perturbation keeps going in both directions near the MPP, and thus, oscillations occur in the power of PV module. Unlike P&O, the slope of the power-against-voltage (P–V) curve of PV module is used by the incremental conductance algorithm to vary the duty cycle of the converter [6], [27]. By varying the duty cycle of the converter, the voltage of the PV module is able to be increased or decreased and thus the PV system is able to operate at the peak of the P–V curve. In actual operation, the PV module rarely operates at the peak of the P–V curve due to the truncation error in the numerical differentiation inside the microcontroller. Thus, permitted error is required in the algorithm [27], [28]. Apart from that, both the conventional P&O and incremental conductance algorithms vary the duty cycle in fixed step size. When there is variation in the solar irradiation level or load resistance, the responses of fixed step size algorithm are slow. Hence, variable step size algorithms are introduced [22], [29], [30]. These algorithms use the slope of the P–V curve in the duty cycle perturbation. But, the step size becomes smaller when the algorithms close to the peak of the P–V curve, and the convergence of the system is also slower.

A few modified algorithms have been introduced to improve the converging speed during the variation in solar irradiation level and load. The relationship between the load line and the MPP locus is used in [31]–[33] to present a fast-converging algorithm. The MPP locus is a line which approximately connects all the MPP for all levels of solar irradiation. In [31] and [32], a control loop is introduced to ensure the PV system operates in accordance with the MPP locus and thus the MPP searching time is reduced. However, tuning is required in the control loop, and it further complicates the MPPT system. In [33], the control loop is eliminated, but the short circuit current and open circuit voltage are required. Thus, disconnection of PV module is required to collect the data and the power is wasted during disconnection. Although the aforementioned

Manuscript received March 19, 2014; revised August 22, 2014 and October 16, 2014; accepted November 19, 2014. Date of publication December 04, 2014; date of current version February 02, 2015. This work was supported in part by the High Impact Research-Ministry of Higher Education (HIR-MOHE) Project UM.C/HIR/MOHE/ENG/17, and in part by the Fundamental Research Grant Scheme (FRGS) under Grant FP014-2014A. Paper no. TII-14-0607.

The authors are with the Power Electronics and Renewable Energy Research Laboratory (PEARL), Department of Electrical Engineering, University of Malaya, Kuala Lumpur 50603, Malaysia (e-mail: koksoon@um.edu.my; saad@um.edu.my).

Color versions of one or more of the figures in this paper are available online at http://ieeexplore.ieee.org.

Digital Object Identifier 10.1109/TII.2014.2378231

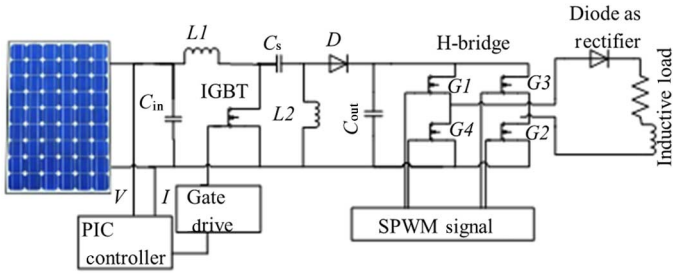

Fig. 1. Proposed PV system with MPPT controller.

algorithms can provide fast response, the complexity of the systems is greatly increased. Therefore, this paper proposes a modified MPPT algorithm, i.e., able to provide fast response without the requirement of an extra control loop.

Other than that, the proposed system also does not require the intermittent disconnection. The proposed PV system simply consists of a dc–dc converter which connected in between the PV module and load. Then, the current and voltage of the PV module are sensed by a PIC controller, which is also used to execute the modified MPPT algorithm. An inverter and a rectifier are connected at the output of the dc–dc converter to validate the proficiency of the proposed algorithm under a nonlinear load. Fig. 1 shows the block diagram of the proposed PV system.

II. Characteristic of PV System With DC–DC Converter

A PV module consists of numbers of solar cell connected in series or parallel and the total power generated is the sum of the power contributed by all of the individual solar cells. A few methods exist in modeling the PV cell [34]–[37], and the model in [36] is used to model the PV cell in this paper. Under different levels of solar irradiation, the PV module produces different levels of power. Fig. 2 shows the I–V curve of PV module under different levels of solar irradiation and also the MPPs which can be connected approximately by a straight line (MPP line) [33]. A load line is generated and it can be imposed on the I–V curve when the PV module supplies power to the load. The power generated by the PV module is the product of the voltage and current of PV module at the intersection point between the load line and the I–V curve. Therefore, the output power of PV module varies according to the solar irradiation (I–V curve) and the resistance of the load (load line). Generally, a dc–dc converter is connected in between the PV module and the load. Then, the MPPT controller is used to regulate the duty cycle of the dc–dc converter to ensure the load line always cuts through the I–V curve at MPP. Thus, the variation in the voltage and current of PV module during the variation in solar irradiation or load as shown in Table I must be considered by the MPPT controller. If the duty cycle of dc–dc converter is fixed, the variation in solar irradiation will either increase or decrease both the voltage and current of PV module simultaneously. Meanwhile, load variation will increase (decrease) the voltage and decrease (increase) the current of PV module. Variations in the voltage and current are always in the opposite direction under load variation. The MPPT controller should only regulates the duty

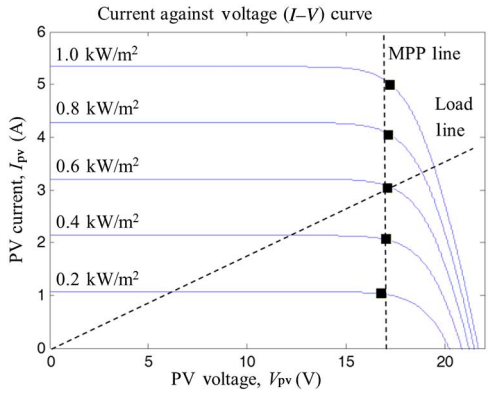

Fig. 2. MPP line and load line on the I–V curves for different levels of solar irradiation.

TABLE I
Variation in the Voltage and Current of the PV Module During the Variation in Solar Irradiation and Load Resistance

		Variation of voltage (dV)	Variation of current (dI)
Solar irradiation	Increase	Positive	
	Decrease	Negative	
Load resistance	Increase	Positive	Negative
	Decrease	Negative	Positive

cycle of dc–dc converter after the variation in solar irradiation or load is determined.

The relationships of the voltage and current of the dc–dc converter between the input and output sides are shown in (1) and (2). The single-ended primary-inductor converter (SEPIC) is used in this paper. Thus, (1) and (2) are specifically required for SEPIC which operates in continuous-conduction mode and may be different for other types of converter. Equation (3) shows that the duty cycle can be regulated to force the input resistance (load line) of the converter to be varied until the load line cuts through the I–V curve at MPP

$$V_{\text{in}} = \frac{1-D}{D} V_{\text{out}} \tag{1}$$

$$I_{\text{in}} = \frac{D}{1-D} I_{\text{out}}. \tag{2}$$

Equation (1) is then divided by (2) to obtain (3) as follows:

$$R_{\text{in}} = \frac{(1-D)^2}{D^2} R_{\text{out}} \tag{3}$$

where V_{in} is the input voltage of the converter or the voltage of the PV module V_{pv}, I_{in} is the input current of the converter or the current of the PV module I_{pv}, R_{in} is the input resistance of the converter or the resistance seen by the PV module, and R_{out} is the output resistance of the converter or load resistance R_{load}.

III. Proposed Modified MPPT Algorithm

The proposed algorithm adopts the relationship between the load line and the I–V curve to introduce a fast-converging algorithm. In the proposed system, only the voltage and current of PV module are sensed by the MPPT controller.

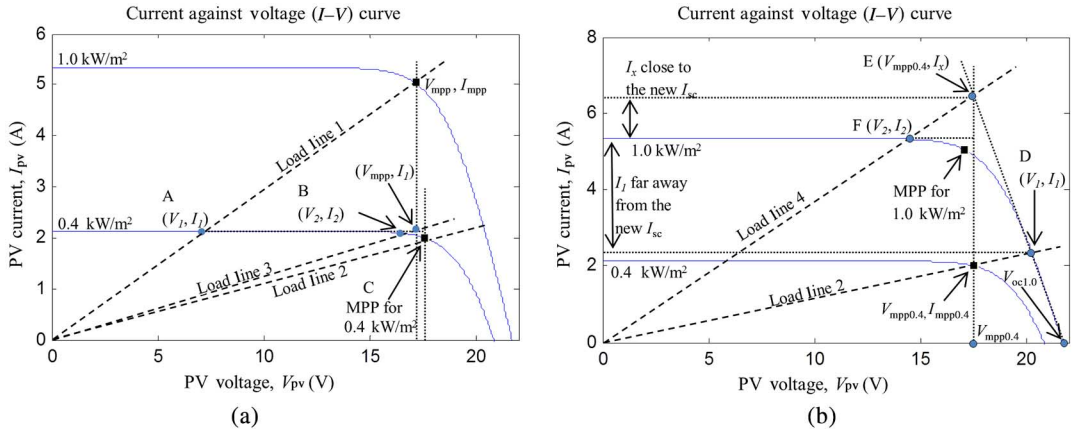

Fig. 3. Load lines on I–V curves for solar irradiation level of 0.4 and $1.0\,\mathrm{kW/m^2}$ during (a) decrease of solar irradiation and (b) increase of solar irradiation.

In the PV system, (3) can be rewritten to obtain (4) and (5) as follows:

$$\frac{V_{\mathrm{pv}}}{I_{\mathrm{pv}}} = \frac{(1-D)^2}{D^2} R_{\mathrm{load}} \tag{4}$$

$$R_{\mathrm{load}} = \frac{D^2}{(1-D)^2} \frac{V_{\mathrm{pv}}}{I_{\mathrm{pv}}}. \tag{5}$$

Under any operating point, the load resistance can be calculated by substituting the duty cycle, voltage, and current of PV module into (5). After the value of load resistance is obtained, (5) can be rewritten into (7). Then, the duty cycle can be calculated by substituting the desired voltage (V_{mpp}) and current (I_{mpp}) of PV module into (7) as follows:

$$\frac{D^2}{(1-D)^2} = \frac{I_{\mathrm{pv}}}{V_{\mathrm{pv}}} R_{\mathrm{load}} \tag{6}$$

$$D = \frac{\sqrt{a}}{1+\sqrt{a}} \tag{7}$$

where $a = \frac{I_{\mathrm{pv}}}{V_{\mathrm{pv}}} R_{\mathrm{load}}$.

In the proposed algorithm, the load of the PV system is calculated by using (5). Then, (7) is used to ensure that the system responds rapidly and operates near to the new MPP whenever there is variation in solar irradiation. For the case of load variation, (5) is used to calculate the new load resistance, then V_{mpp} and I_{mpp} are substituted into (7) to obtain the new duty cycle.

A. Decrease in Solar Irradiation Level

If the PV module operates at load line 1 and the solar irradiation is $1.0\,\mathrm{kW/m^2}$, the current and voltage of PV module are V_{mpp} and I_{mpp} as shown in Fig. 3(a). Then, if the solar irradiation decreases to $0.4\,\mathrm{kW/m^2}$, while the duty cycle of the dc–dc converter remains unchanged, the operating point of PV module is at point A (V_1, I_1) of load line 1 which is far away from the MPP of $0.4\,\mathrm{kW/m^2}$, point C in Fig. 3(a). In order to perturb the operating point of the PV module to the new MPP by using (7), the voltage and current of the new MPP is required. However, these two values are unknown. Therefore, approximated values are substituted into (7) to ensure the PV module operates near to the new MPP. As shown in Fig. 3(a), the current of point A, I_1 is close to the short circuit current of $0.4\,\mathrm{kW/m^2}$ and the current of MPP is always approximately $0.8 * I_{\mathrm{sc}}$. Thus, I_1 is approximated as the current of new MPP. Then, Fig. 2 shows the voltages of MPP for each level of solar irradiations are closed to one another. Hence, the previous MPP voltage, V_{mpp} is approximated as the voltage of new MPP. Subsequently, V_{mpp} and I_1 are substituted into (7) to perturb the operating point of PV module to load line 3, point B (V_2, I_2) which is near to the new MPP. With only single perturbation, the operating point of the PV module converged from point A to point B rapidly. Finally, a few more steps of conventional incremental conductance algorithm are used to track the new MPP, point C. Therefore, the convergence time from point A to point C is greatly reduced.

B. Increase in Solar Irradiation Level

If the PV module operates at load line 2 and the solar irradiation is $0.4\,\mathrm{kW/m^2}$, the current and voltage of the PV module are $V_{\mathrm{mpp0.4}}$ and $I_{\mathrm{mpp0.4}}$ as shown in Fig. 3(b). Then, if the solar irradiation increases to $1.0\,\mathrm{kW/m^2}$, while the duty cycle of the dc–dc converter remains unchanged, the operating point of PV module is at point D (V_1, I_1) of load line 2 which is far away from the MPP of $1.0\,\mathrm{kW/m^2}$. Similar to the algorithm used in the case of decrease in solar irradiation level, the approximated values are substituted into (7) to ensure the PV module operates near to the new MPP. However, the operating current, I_1 is far away from the short circuit current of $1.0\,\mathrm{kW/m^2}$ as shown in Fig. 3(b). Thus, an additional step is required to ensure the operating current of PV module is near to the I_{sc} of new MPP. As shown in Fig. 3(b), point E, $V_{\mathrm{oc1.0}}$, and $V_{\mathrm{mpp0.4}}$ form a right-angled rectangle.

By applying the trigonometry rule in (8), the operating current I_x, which is near to the I_{sc} of $1.0\,\mathrm{kW/m^2}$ is obtained. The open circuit voltage V_{oc} of the PV module in (9) is the approximated open circuit voltage obtained from $V_{\mathrm{mpp}}/0.8$. Then, V_{mpp} is the voltage of the MPP before the variation in solar irradiation. V_1 is the voltage of PV module after the variation in solar irradiation

$$\frac{V_1 - V_{\mathrm{mpp}}}{I_x - I_1} = \frac{V_{\mathrm{oc}} - V_{\mathrm{mpp}}}{I_x}. \tag{8}$$

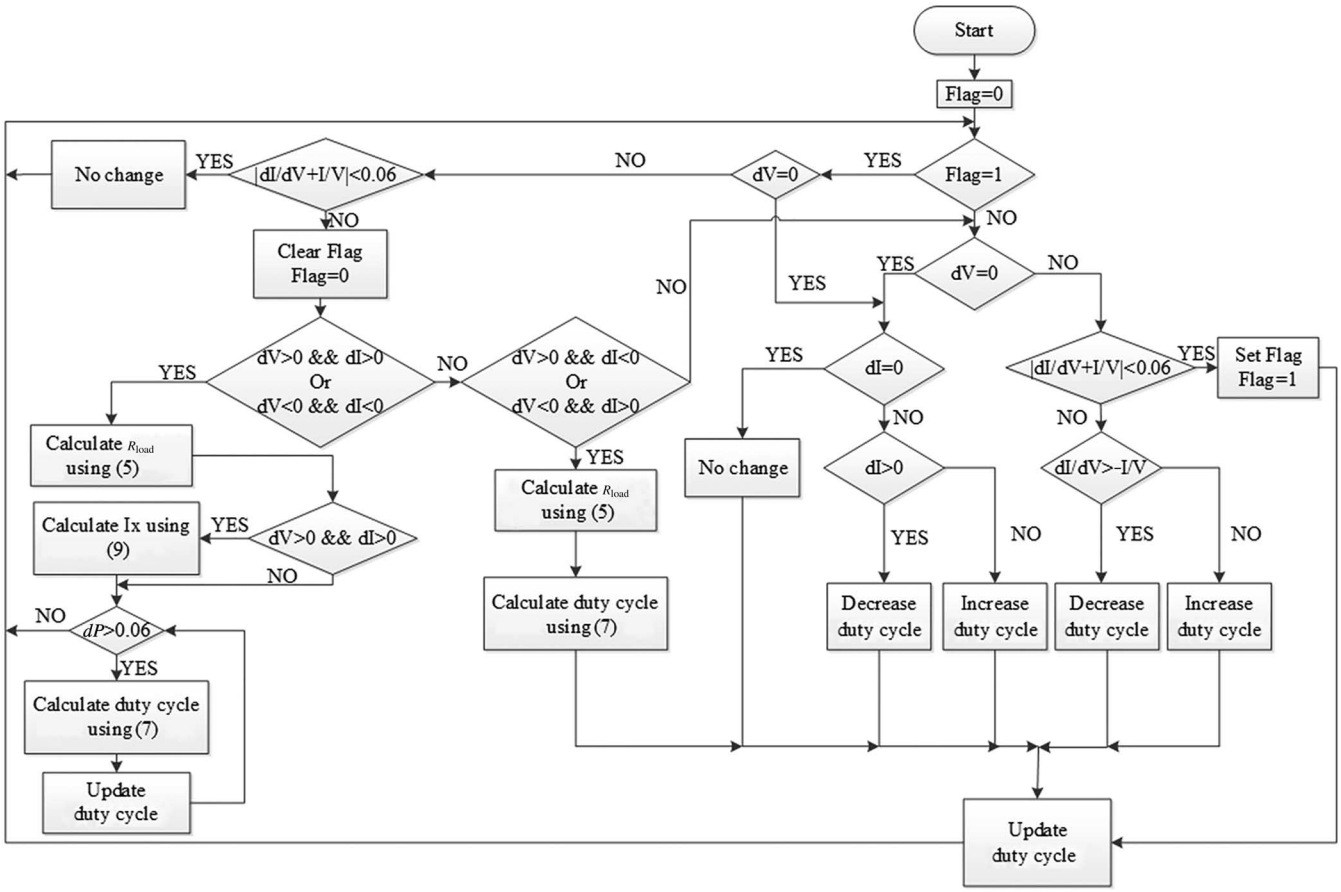

Fig. 4. Flowchart of the proposed MPPT algorithm.

Equation (8) is rearranged to obtain (9)

$$I_x = \frac{V_{\rm oc} - V_{\rm mpp}}{V_{\rm oc} - V_1} I_1. \tag{9}$$

In the second step, I_x and the voltage of the previous MPP $V_{\rm mpp0.4}$ are substituted into (7) to obtain the new duty cycle. With the new duty cycle, the PV module operates at point F (V_2, I_2) of load line 4, which is close to the new MPP at $1.0\,{\rm kW/m^2}$. Then, the conventional incremental conductance algorithm is used to track the MPP.

C. Load Variation

Table I is used to identify the existence of load variation. After the load variation, the operating point of the PV module diverts from the MPP (load line no longer cut through MPP). A new duty cycle is required to ensure the PV module operates at the MPP again (load line cut through MPP). As variation only exists in the load, the voltage and current at the MPP should be the same (I–V curve unchanged). Thus, (5) is used to obtain the new resistance of the load. Then, by substituting the voltage and current at the MPP into (7), the new duty cycle can be calculated. With the new duty cycle, the PV module operates at the point close to the MPP and then, the conventional algorithm is used to track the MPP.

Fig. 4 shows the flowchart for the proposed algorithm. A flag value is used to indicate that the PV system is operating at the MPP if it is set to 1. Therefore, the flag is set to 0 initially. Then, the conventional incremental conductance algorithm is used to track the MPP. A permitted error of 0.06 as shown in (10), is used in the proposed algorithm to eliminate the steady-state oscillation in the system after the MPP is reached. The permitted error is chosen based on the duty cycle step size (0.005), and the accuracy in the power of the PV module at MPP is $\pm 0.7\%$

$$\left| \frac{dI}{dV} + \frac{I}{V} \right| < 0.06. \tag{10}$$

After the algorithm tracked the MPP, the flag is set to 1, and the program is loaded into the proposed algorithm. Then, (10) is checked, and the duty cycle does not regulated if (10) is satisfied. When the solar irradiation or load is varied, (10) no longer holds and the flag is set to 0. Then, the resistance of the load is calculated by using (5) and the direction of variation in the solar irradiation or load is determined. If both the current and voltage of the PV module are decreased, (7) is used to calculate the new duty cycle. If both the current and voltage of the PV module are increased, I_x is calculated by using (9), and then, the new duty cycle is calculated by using (7). In the case of a nonlinear load, the response of the system is slower (the PV system is unable to operate near to the new MPP in single perturbation). Thus, changes in the power of the PV module are monitored. If the power of the PV module increases after the perturbation in duty cycle, (7) is used to calculate the new duty cycle again. Until the difference in power (dP) is smaller than 0.06, only then the conventional algorithm is applied. Meanwhile, for load

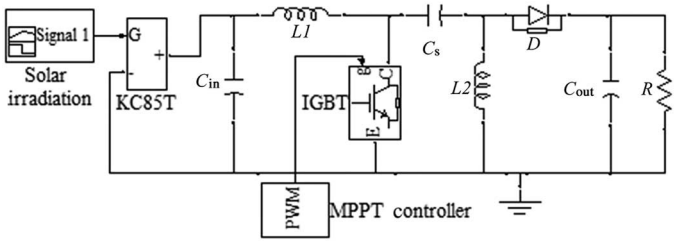

Fig. 5. MATLAB simulation model of MPPT controller and SEPIC converter.

TABLE II
PARAMETER OF THE KC85T PV MODULE AT STC: TEMPERATURE $= 25°\mathrm{C}$ AND INSOLATION $= 1000\,\mathrm{W/m^2}$

Maximum power (P_{max})	87 W
Voltage at MPP (V_{mpp})	17.4 V
Current at MPP (I_{mpp})	5.02 A
Open circuit voltage (V_{oc})	21.7 V
Short circuit current (I_{sc})	5.34 A

variation, the new duty cycle is calculated by using (7) after the resistance of the load is obtained by (5).

IV. Simulation Results

Fig. 5 shows the MATLAB Simulink model of the MPPT system consisting of the PV module, SEPIC, MPPT controller, and load. The specifications of the PV module are shown in Table II. The values of the components in the SEPIC are as follows: C_{in} and $C_{\mathrm{out}} = 3900\,\mu\mathrm{F}$, L_1 and $L_2 = 125\,\mu\mathrm{H}$, $C_s = 1000\,\mu\mathrm{F}$, and the load is a $10\,\Omega$ resistance. The switching frequency for the insulated-gate bipolar transistor (IGBT) is set to 20 kHz.

A. Solar Irradiation Variation

Simulation for the proposed algorithm and conventional incremental conductance algorithm are carried out, and the results are compared. Sampling time for the MPPT controller is 0.05 s, and step size of the duty cycle is 0.005 (duty cycle step size for conventional incremental conductance algorithm). Simulation time is 4 s, and solar irradiation level varies from low ($0.4\,\mathrm{kW/m^2}$) to high ($1.0\,\mathrm{kW/m^2}$) and then reduced to low again in order to investigate the performance of the system under fast-varying solar irradiation level.

1) Conventional Incremental Conductance Algorithm: Fig. 6(a) shows the results of the simulation for conventional incremental conductance algorithm. Initially, the solar irradiation level is set to $0.4\,\mathrm{kW/m^2}$. Then, the algorithm tracked the MPP at $t = 0.25\,\mathrm{s}$, and the duty cycle of the converter is fluctuating between 0.525 and 0.535. Thus, the power of the PV module is also fluctuating around the MPP (35.09–35.14 W), and the PV module operates at around load line 2 (point A), as shown in Fig. 7(a). Then, the solar irradiation level is increased to $1.0\,\mathrm{kW/m^2}$ at $t = 0.68\,\mathrm{s}$ while the duty cycle of the converter is at 0.535, and the PV module operates at load line 2 (point B). At $t = 0.7\,\mathrm{s}$, the duty cycle of the converter is increased by the MPPT controller step by step until the MPP for $1.0\,\mathrm{kW/m^2}$ is reached at $t = 1.9\,\mathrm{s}$. The duty cycle and the power (86.06–86.38 W) of the PV module are fluctuating around the MPP. As the solar irradiation level increases, a total time of 1.2 s is required to reach the MPP and the PV system operates at around load line 1 (point C), as shown in Fig. 7(a). After that, the solar irradiation level is decreased to $0.4\,\mathrm{kW/m^2}$ at $t = 2.48\,\mathrm{s}$, and the PV module operates at load line 1 (point D), as shown in Fig. 7(a). After the MPPT controller samples at 2.5 s, the duty cycle of the converter is decreased step by step. At $t = 3.5\,\mathrm{s}$, the MPP is reached, and the PV module operates at around load line 2 (point A), as shown in Fig. 7(a), and the power of the PV module is fluctuating around the MPP (35.09–35.14 W). The searching time for the PV system to reach the new MPP at $0.4\,\mathrm{kW/m^2}$ is 1.0 s.

2) Proposed MPPT Algorithm: Fig. 6(b) shows the simulation results for the proposed algorithm. Initially, the irradiation level is $0.4\,\mathrm{kW/m^2}$. Conventional incremental conductance algorithm is used to track the MPP, and it is tracked at $t = 0.15\,\mathrm{s}$. By using (10), the PV module operates at load line 2 (point E), as shown in Fig. 7(b). The duty cycle of the converter remains constant at 0.525, and the power of the PV module is fixed at 35.04 W. After the MPP is tracked, the flag value is set to 1, and no variation in the duty cycle until a variation in the solar irradiation level is found at $t = 0.68\,\mathrm{s}$. After the solar irradiation is increased to $1.0\,\mathrm{kW/m^2}$, the PV module operates at point F. At $t = 0.7\,\mathrm{s}$, the MPPT controller detected the increased in both the current and voltage of the PV module. Hence, (5) is used to calculate the resistance of the load, and then, (9) and (7) are used to calculate I_x as well as the new duty cycle. With the new duty cycle, the PV module operates at load line 4 (point G), as shown in Fig. 7(b). As the power of the PV module has been increased ($\mathrm{dP} > 0.06$), the proposed algorithm continues to perturb the duty cycle by substituting I_x and voltage of the PV module into (7). After that, the controller detected the drop in the power of the PV module ($\mathrm{dP} < 0.06$) at point H, and thus the conventional incremental conductance algorithm is used to track the MPP for $1.0\,\mathrm{kW/m^2}$ at load line 1 (point I) at $t = 1.0\,\mathrm{s}$. A total searching time of 0.3 s is required to reach the new MPP. The duty cycle remains constant at 0.637, and the power of the PV module is at 86.28 W. At $t = 2.48\,\mathrm{s}$, the solar irradiation level decreases to $0.4\,\mathrm{kW/m^2}$, and the PV module operates at load line 1 (point J), as shown in Fig. 7(b). At $t = 2.5\,\mathrm{s}$, the MPPT controller is sampled, (5) and (7) are used to obtain the resistance of the load and the new duty cycle. With the new duty cycle, the PV module operates at point K, which is near to the MPP for $0.4\,\mathrm{kW/m^2}$. The algorithm continues to modulate the duty cycle by using (7) because $\mathrm{dP} > 0.06$. At $t = 2.75\,\mathrm{s}$, the algorithm detected the $\mathrm{dP} < 0.06$, and thus, the perturbation stops and MPP (point E) is tracked. Then, the flag is set to 1. The duty cycle (0.53) and the power of PV module (35.14 W) are fixed. For the decrease in solar irradiation level, the MPP searching time is 0.25 s.

B. Load Variation

Fig. 8 shows the simulation results for the conventional incremental conductance and proposed algorithms during the load

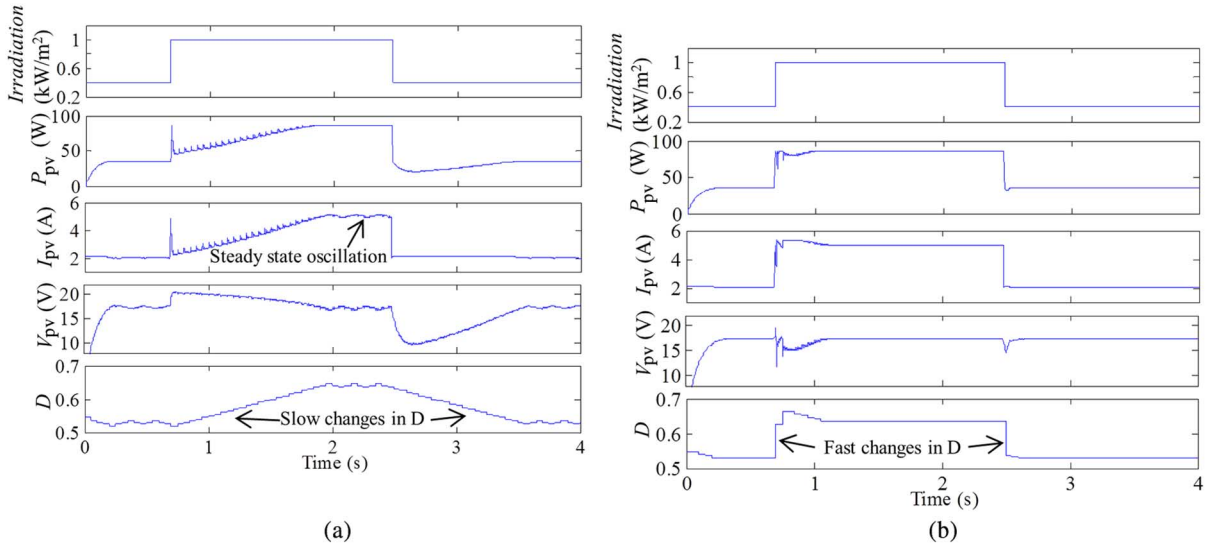

Fig. 6. Waveforms of PV power, current, voltage, and duty cycle during variation in solar irradiation level. (a) Conventional incremental conductance algorithm. (b) Proposed algorithm.

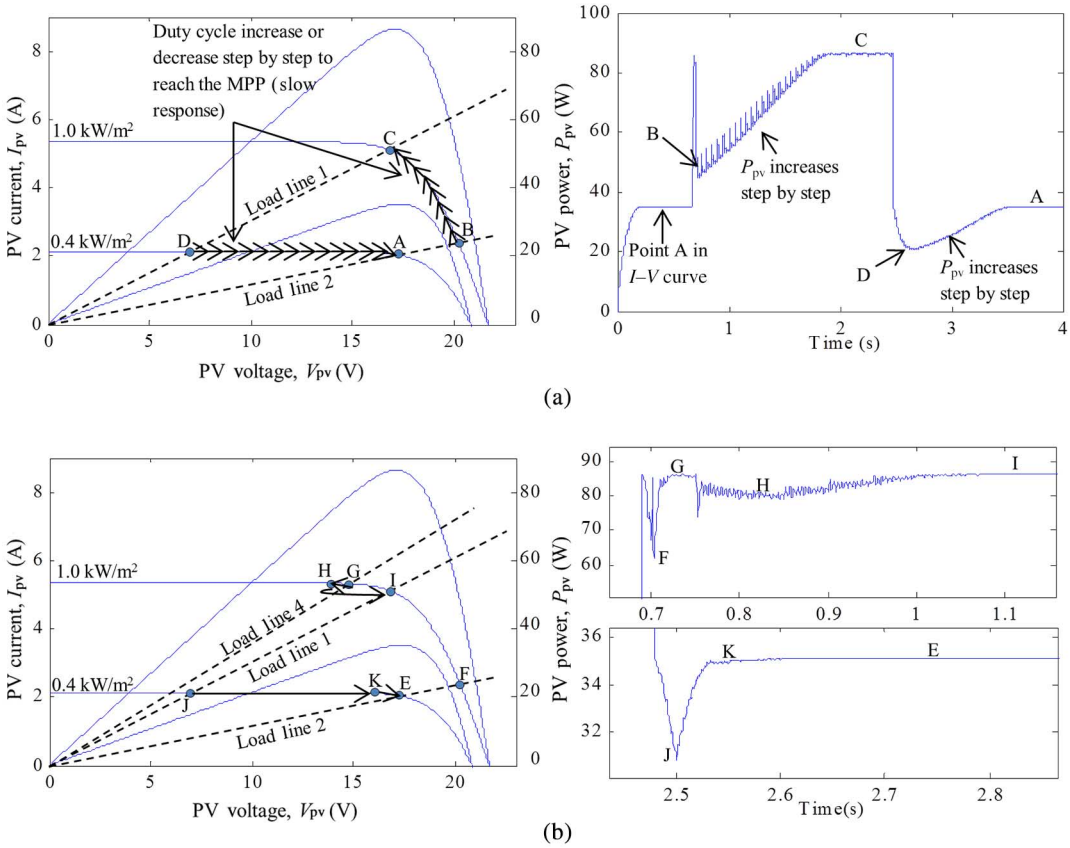

Fig. 7. I–V curve, P–V curve, and power waveform during variation in solar irradiation level. (a) Conventional incremental conductance algorithm. (b) Proposed algorithm.

variation. Initially, the resistance of the load is at $14\,\Omega$, and then at $t = 0.6\,\text{s}$, the resistance is decreased to $10\,\Omega$. After that, the resistance is increased to $14\,\Omega$ again at $t = 1.2\,\text{s}$. As shown in the power waveforms, the proposed algorithm responds faster than the conventional incremental conductance algorithm. Initially, the MPP is tracked at $t = 0.3\,\text{s}$, and the V_{mpp} and I_{mpp} are saved in the memory of the PIC controller. When the algorithm detected the variation in the load, (5) is used to calculate the resistance of the load. Then, the voltage and current at the MPP (V_{mpp} and I_{mpp}) are substituted into (7) to calculate the new duty cycle. During the decrease in the resistance of the load, 0.2 s is required by the proposed algorithm to regulate the operating point of the PV module back to the MPP. Then, 0.05 s is required during the increase in

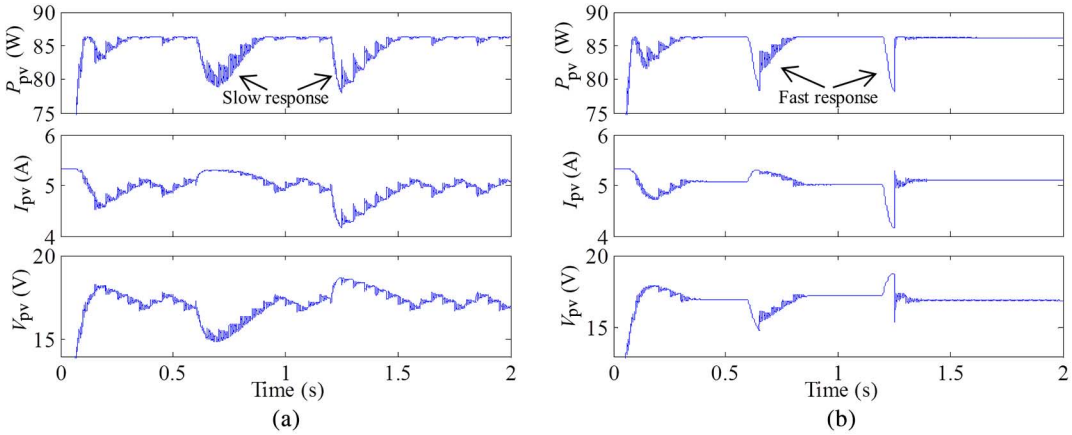

Fig. 8. Waveforms of power, voltage, and current of PV module during variation in load. (a) Conventional incremental conductance algorithm. (b) Proposed algorithm.

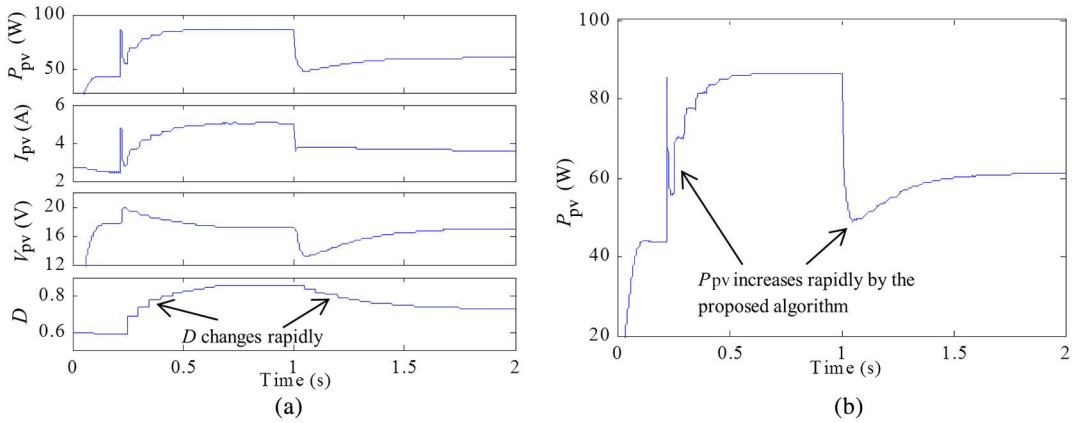

Fig. 9. (a) Waveforms of PV power, current, voltage, and duty cycle during variation in solar irradiation level when nonlinear load is connected. (b) Enlarged view of power waveform.

the resistance of the load. Meanwhile, 0.25 s is required by the conventional incremental conductance algorithm during the decrease and increase in the resistance of the load, respectively.

C. Nonlinear Load

To ensure that the proposed algorithm is able to function accurately even in a nonlinear load, the inverter and rectifier have been added into the simulation. H-bridge inverter has been used in the simulation, and sinusoidal pulse-width modulation with 10 kHz of carrier frequency is implemented. The inverter output is in 50 Hz (modulation index, $m_f = 200$). Then, the output load of the inverter is an inductive load (10 Ω and 0.3 H). Fig. 9 shows the simulation results. Initially, the irradiation of the PV module is at $0.5\,\mathrm{kW/m^2}$, and the MPP is tracked by using the conventional incremental conductance algorithm at $t = 0.1\,\mathrm{s}$ ($\mathrm{duty\,cycle} = 0.59$ and $P_{\mathrm{pv}} = 43.92\,\mathrm{W}$). Then, the solar irradiation increases to $1.0\,\mathrm{kW/m^2}$ at $t = 0.22\,\mathrm{s}$. The MPPT controller observed the increased in both the current and voltage of the PV module. Therefore, (5) is used to calculate the resistance of the load, and then, (7) is used to obtain the new duty cycle. However, because of the nonlinear load, the response of the system is not as fast as the case of resistive load. Therefore, the controller keeps on updating the duty

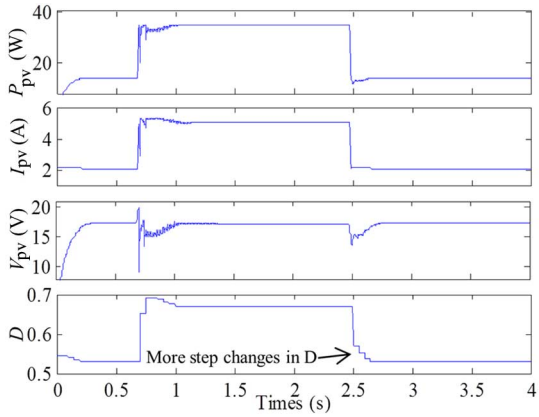

Fig. 10. Simulation results for the simultaneous variation in solar irradiation and load.

cycle of the converter by substituting I_x and the voltage of PV module into (7). Until at $t = 0.65\,\mathrm{s}$, the perturbation is stopped after $\mathrm{dP} < 0.06$, and the MPP is tracked by the controller ($\mathrm{duty\,cycle} = 0.85$ and $P_{\mathrm{pv}} = 86.37\,\mathrm{W}$). At $t = 1.01\,\mathrm{s}$, the solar irradiation is decreased to $0.7\,\mathrm{kW/m^2}$. The MPPT controller modulated the duty cycle by using (7) and tracked the MPP at $t = 1.8\,\mathrm{s}$ ($\mathrm{duty\,cycle} = 0.72$ and $P_{\mathrm{pv}} = 61\,\mathrm{W}$).

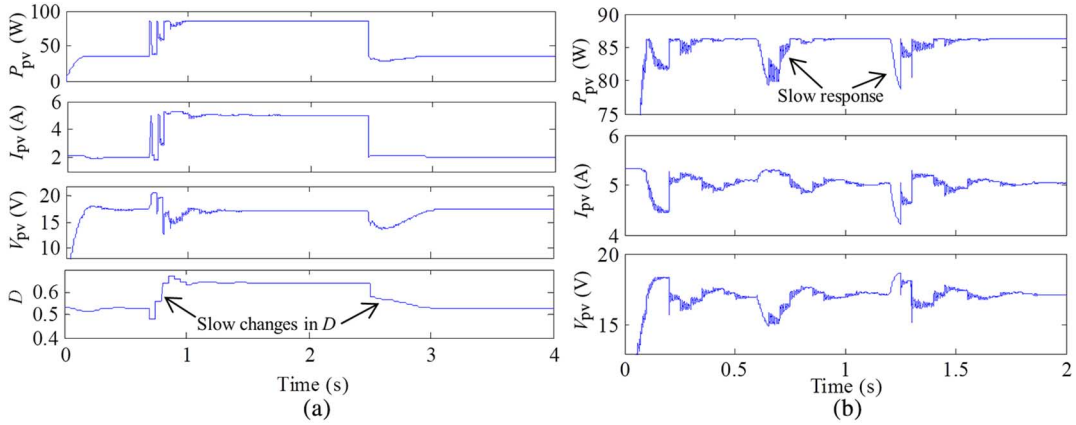

Fig. 11. Simulation results for the variable step size incremental conductance algorithm. (a) Solar irradiation variation. (b) Load variation.

TABLE III
COMPARISON BETWEEN CONVENTIONAL INCREMENTAL CONDUCTANCE ALGORITHM AND PROPOSED ALGORITHM

Evaluated parameters	Conventional algorithm	Variable step size algorithm [29]	Proposed algorithm
Tracking speed (s)	1.1	0.4	0.275
Steady state oscillation	Large	Small	No
Execution time during load variation (s)	0.5	0.5	0.3
Practical implementation	Yes	Yes	Yes
Power efficiency	Low	Medium	High

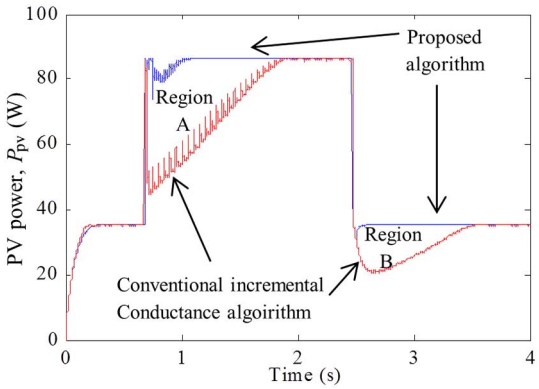

Fig. 12. Power waveforms for both conventional and proposed algorithm during solar irradiation variation.

D. Simultaneous Variation in Solar Irradiation and Load

Fig. 10 shows the results of the proposed algorithm under simultaneous variation in solar irradiation and load. Initially, the solar irradiation is $0.4\,\mathrm{kW/m^2}$ and the load is $10\ \Omega$. The MPP is tracked at $t = 0.15\,\mathrm{s}$. At $t = 0.68\,\mathrm{s}$, the solar irradiation is increased to $1.0\,\mathrm{kW/m^2}$ and at the same time, the load is also increased to $14\ \Omega$. The simulation results show that the proposed algorithm is able to track the MPP for $1.0\,\mathrm{kW/m^2}$ accurately and the time consumed is 0.3 s. Then at $t = 2.47\,\mathrm{s}$, the solar irradiation and load is decreased back to $0.4\,\mathrm{kW/m^2}$ and $10\ \Omega$. The proposed algorithm is also able to track the MPP accurately and the time consumed is 0.2 s. Thus, the proposed algorithm is also able to work under simultaneous variation in solar irradiation and load.

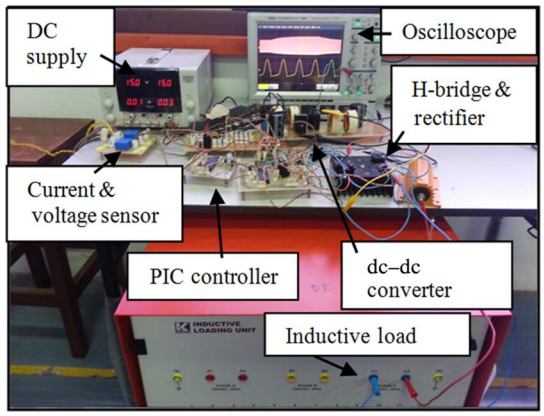

Fig. 13. Experimental setup for the proposed PV system.

E. Variable Step Size Incremental Conductance Algorithm

Apart from the conventional incremental conductance algorithm, the simulation for the variable step size incremental conductance algorithm [29] is also carried out under the same solar irradiation and load variation. Fig. 11(a) shows the variable step size algorithm requires 0.3 s to reach the MPP during the increase in the solar irradiation and 0.5 s to reach the MPP during the decrease in solar irradiation. On average, 0.4 s is required by the variable step size algorithm during solar irradiation variation. Fig. 11(b) shows the variable step size algorithm requires 0.3 s to reach back to the MPP during the decrease in load and 0.2 s during the increase in load. On average, 0.25 s is required by the variable step size algorithm during the load variation.

Table III shows the comparison between the conventional incremental conductance algorithm, variable step size algorithm, and the proposed algorithm. From the simulation results, the average tracking time required by the conventional and variable step size algorithms during the variation in solar irradiation level is 1.1 s and 0.4 s, but the proposed algorithm only requires 0.275 s. Therefore, the proposed algorithm is four times faster than the conventional algorithm. Furthermore, the

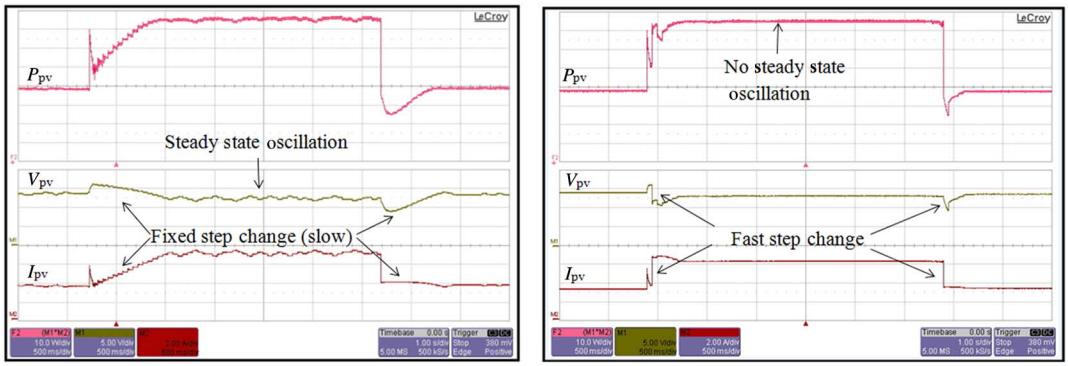

Fig. 14. Experimental results with resistive load for (a) conventional incremental conductance algorithm and (b) proposed algorithm.

proposed algorithm is also 1.6 times faster than the conventional and variable step size algorithms during load variation. Meanwhile, for a nonlinear load during the increase in solar irradiation, the duty cycle changed from 0.59 to 0.85, and the total time required by the proposed algorithm is 0.3 s. For the conventional algorithm, the total time required to perturb the duty cycle from 0.59 to 0.85 is 2.5 s ($\text{duty cycle step size} = 0.005$ and $\text{sample time} = 0.05$ s). The conventional algorithm showed steady-state oscillation about 0.37 W in the power of PV module, but the proposed algorithm does not have steady-state oscillation. Fig. 12 shows the power waveforms for proposed and conventional incremental conductance algorithms. By using the proposed algorithm, the amount of energy losses, which can be reduced during the increase in solar irradiation level, is about 23 J (Region A), and for the decrease in solar irradiation level is about 6.6 J (Region B). As shown in the simulation results, the proposed algorithm is able to provide fast and accurate response during the variation in solar irradiation and load. Thus, the efficiency of the PV system is able to be increased as shown in Fig. 12.

V. Experimental Results

The hardware was constructed according to the simulation specifications. The PIC controller PIC18f4520 from Microchip was used to implement the control algorithm. The PIC consists of 10-bit analog-to-digital converters which, used to convert the voltage and current of PV module. Current (LA25-NP) and voltage (LV25-P) sensor from Liaisons Electroniques-Mecaniques (LEM) were used to sense the voltage and current of PV module before sending it to the PIC controller. In the MPPT controller, the switching frequency of the dc–dc converter is only 20 kHz and thus the IGBT is chosen as the switching device [38]. The experimental setup is shown in Fig. 13.

A. Solar Irradiation Variation

PV modules are used in the experimental setup to obtain the sudden variation in the solar irradiation level. The increase (step change) in solar irradiation level can be created by connecting two PV modules in parallel. As in the simulation, initially, a PV module is connected to the input of the SEPIC. After the MPP is reached, the second PV module is connected in parallel to determine the responses of the MPPT algorithms toward the increase in solar irradiation level. Then, the second PV module is disconnected to obtain the response on the decrease in solar irradiation level. Fig. 14 shows the power, current, and voltage of the PV module. The step change in the solar irradiation is the same as in the simulation, and the experimental results obtained are similar to the simulation results. The proposed algorithm is able to track the MPP in a few step changes in the duty cycle, and no steady-state oscillation is found after the MPP is tracked. Meanwhile, the conventional algorithm requires a longer time to track the MPP, and steady-state oscillation is found after the MPP is tracked. Fig. 15 shows the power waveforms of the PV module during the increase and decrease in solar irradiation level. During the sampling of the MPPT controller, (5) is used to obtain the resistance of the load, and then, (7) is used to calculate the new duty cycle. Then, $\mathrm{dP} > 0.06$ and the algorithm continue to update the duty cycle by using (7) until $\mathrm{dP} < 0.06$. Then, the proposed algorithm stops, and a few more steps of conventional algorithm are used to ensure the PV module operates at the MPP. The proposed algorithm can track the MPP faster than the conventional algorithm under fast-varying solar irradiation.

B. Load Variation

Fig. 16 shows the experimental results for load variation, where the results are similar to those in the simulation. The power waveform shows that the proposed algorithm returns to the MPP rapidly as compared to the conventional algorithm. Both of the algorithms regulate the duty cycle to ensure the PV module operates at the MPP when variations are found in the resistance of load, but the proposed algorithm responds to the load variation rapidly and thus improved the efficiency of the PV system.

C. Nonlinear Load

Fig. 17(a) shows the power, voltage, and current waveforms of the PV module when the output is connected to the inverter and rectifier (inductive load, 10 Ω, 0.3 H). The proposed algorithm responds rapidly by using (7) to calculate the duty cycle.

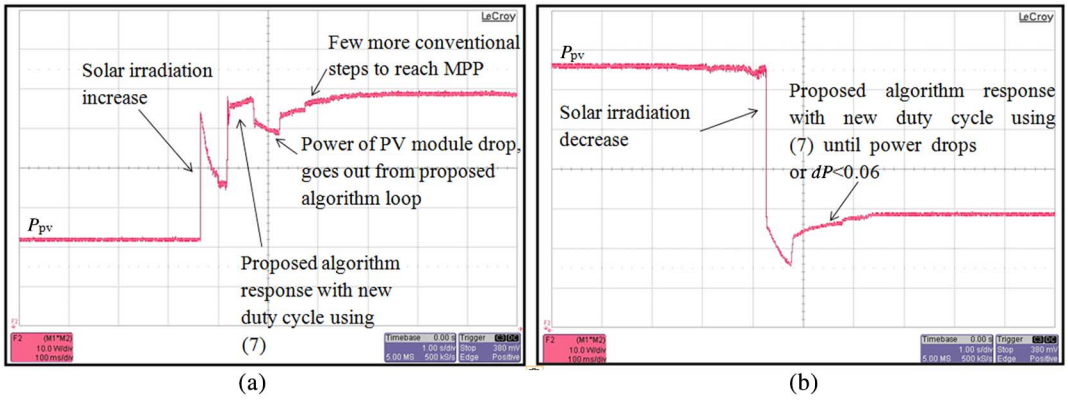

Fig. 15. Zoom-in view of power waveforms during (a) increase in solar irradiation and (b) decrease in solar irradiation.

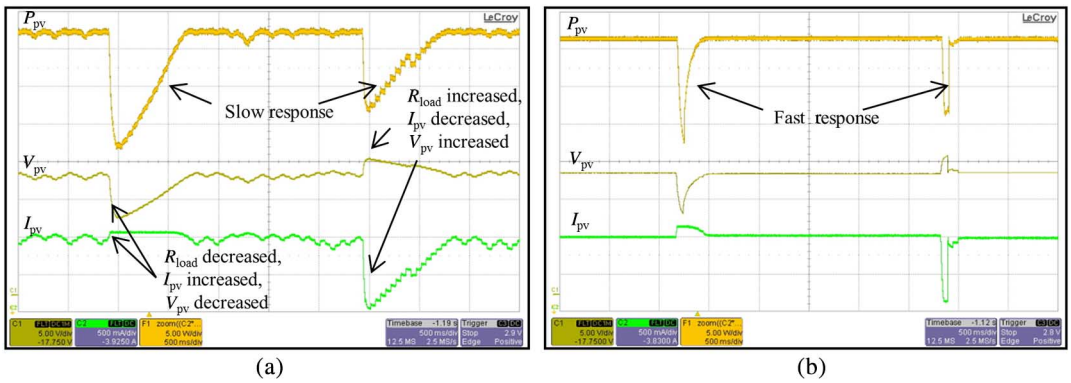

Fig. 16. Waveforms of power, voltage, and current of PV module during load variation. (a) Conventional algorithm. (b) Proposed algorithm.

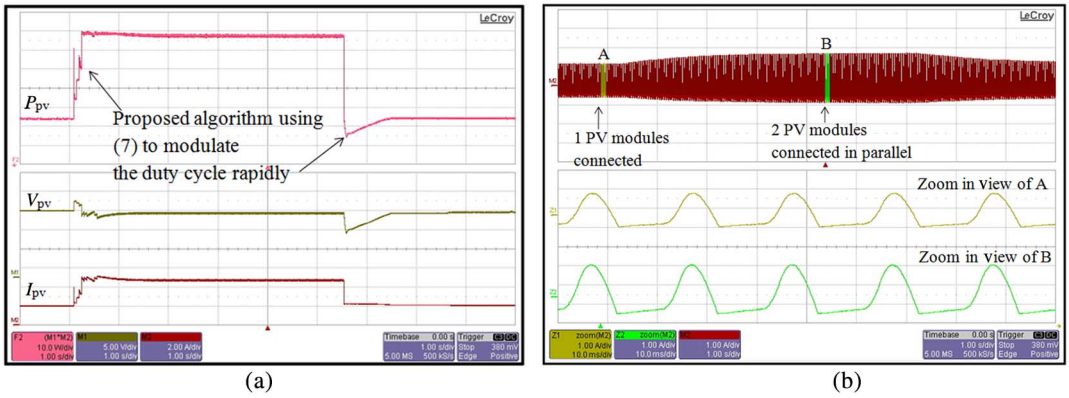

Fig. 17. Experimental results with nonlinear load for proposed algorithm. (a) Power, voltage, and current waveforms of PV module. (b) Rectified current waveforms of inductive load.

Then, the rectified inverter output current waveform is shown in Fig. 17(b). The current increases when the two PV modules are connected in parallel.

VI. Conclusion

The proposed system only requires a dc–dc converter and a PIC microcontroller which is simpler than those which requires extra control loop and intermittent disconnection. Furthermore, the proposed algorithm responds to the variation in solar irradiation and load faster than the conventional algorithm as shown in the simulation and experimental results. In addition, there is no steady-state oscillation in the proposed algorithm and thus reduce the power losses. As a conclusion, a fast converging and low losses MPPT algorithm is proposed and verified experimentally in this paper.

References

[1] S. Mekhilef, R. Saidur, and A. Safari, "A review on solar energy use in industries," *Renew. Sustain. Energy Rev.*, vol. 15, pp. 1777–1790, 2011.
[2] C. Paravalos *et al.*, "Optimal design of photovoltaic systems using high time-resolution meteorological data," *IEEE Trans. Ind. Informat.*, vol. 10, no. 4, pp. 2270–2279, Nov. 2014.

[3] M. N. Kabir, Y. Mishra, G. Ledwich, Z. Y. Dong, and K. P. Wong, "Coordinated control of grid-connected photovoltaic reactive power and battery energy storage systems to improve the voltage profile of a residential distribution feeder," *IEEE Trans. Ind. Informat.*, vol. 10, no. 2, pp. 967–977, May 2014.
[4] R. A. Mastromauro, M. Liserre, and A. Dell'Aquila, "Control issues in single-stage photovoltaic systems: MPPT, current and voltage control," *IEEE Trans. Ind. Informat.*, vol. 8, no. 2, pp. 241–254, Apr. 2012.
[5] E. Mamarelis, G. Petrone, and G. Spagnuolo, "An hybrid digital-analog sliding mode controller for photovoltaic applications," *IEEE Trans. Ind. Informat.*, vol. 9, no. 2, pp. 1094–1103, Jan. 2013.
[6] T. K. Soon and S. Mekhilef, "Modified incremental conductance algorithm for photovoltaic system under partial shading conditions and load variation," *IEEE Trans. Ind. Electron.*, vol. 61, no. 10, pp. 5384–5392, May 2014.
[7] S. Gab-Su, S. Jong-Won, C. Bo-Hyung, and L. Kyu-Chan, "Digitally controlled current sensorless photovoltaic micro-converter for DC distribution," *IEEE Trans. Ind. Informat.*, vol. 10, no. 1, pp. 117–126, Dec. 2014.
[8] C. Liang-Rui, T. Chih-Hui, L. Yuan-Li, and L. Yen-Shin, "A biological swarm chasing algorithm for tracking the PV maximum power point," *IEEE Trans. Energy Convers.*, vol. 25, no. 2, pp. 484–493, May 2010.
[9] L. Yi-Hwa, H. Shyh-Ching, H. Jia-Wei, and L. Wen-Cheng, "A particle swarm optimization-based maximum power point tracking algorithm for PV systems operating under partially shaded conditions," *IEEE Trans. Energy Convers.*, vol. 27, no. 4, pp. 1027–1035, Nov. 2012.
[10] L. Kui-Jun and K. Rae-Young, "An adaptive maximum power point tracking scheme based on a variable scaling factor for photovoltaic systems," *IEEE Trans. Energy Convers.*, vol. 27, no. 4, pp. 1002–1008, Nov. 2012.
[11] R. A. Mastromauro, M. Liserre, and A. Dell'Aquila, "Control issues in single-stage photovoltaic systems: MPPT, current and voltage control," *IEEE Trans. Ind. Informat.*, vol. 8, no. 2, pp. 241–254, Apr. 2012.
[12] T. Esram and P. L. Chapman, "Comparison of photovoltaic array maximum power point tracking techniques," *IEEE Trans. Energy Convers.*, vol. 22, no. 2, pp. 439–449, May 2007.
[13] A. Al Nabulsi and R. Dhaouadi, "Efficiency optimization of a DSP-based standalone PV system using fuzzy logic and dual-MPPT control," *IEEE Trans. Ind. Informat.*, vol. 8, no. 3, pp. 573–584, Jul. 2012.
[14] T. L. Kottas, Y. S. Boutalis, and A. D. Karlis, "New maximum power point tracker for PV arrays using fuzzy controller in close cooperation with fuzzy cognitive networks," *IEEE Trans. Energy Convers.*, vol. 21, no. 3, pp. 793–803, Aug. 2006.
[15] C. Chian-Song, "T-S fuzzy maximum power point tracking control of solar power generation systems," *IEEE Trans. Energy Convers.*, vol. 25, no. 4, pp. 1123–1132, Nov. 2010.
[16] L. Zhang, W. G. Hurley, and W. H. Wölfle, "A new approach to achieve maximum power point tracking for PV system with a variable inductor," *IEEE Trans. Power Electron.*, vol. 26, no. 4, pp. 1031–1037, Jun. 2011.
[17] M. Qiang, S. Mingwei, L. Liying, and J. M. Guerrero, "A novel improved variable step-size incremental-resistance MPPT method for PV systems," *IEEE Trans. Ind. Electron.*, vol. 58, no. 6, pp. 2427–2434, May 2011.
[18] L. Whei-Min, H. Chih-Ming, and C. Chiung-Hsing, "Neural-network-based MPPT control of a stand-alone hybrid power generation system," *IEEE Trans. Power Electron.*, vol. 26, no. 12, pp. 3571–3581, Dec. 2011.
[19] A. Ahmed, L. Ran, S. Moon, and J. H. Park, "A fast PV power tracking control algorithm with reduced power mode," *IEEE Trans. Energy Convers.*, vol. 28, no. 3, pp. 1–11, Aug. 2013.
[20] B. N. Alajmi, K. H. Ahmed, S. J. Finney, and B. W. Williams, "Fuzzy-logic-control approach of a modified hill-climbing method for maximum power point in microgrid standalone photovoltaic system," *IEEE Trans. Power Electron.*, vol. 26, no. 4, pp. 1022–1030, Jun. 2011.
[21] M. A. G. de Brito, L. Galotto, L. P. Sampaio, G. de Azevedo e Melo, and C. A. Canesin, "Evaluation of the main MPPT techniques for photovoltaic applications," *IEEE Trans. Ind. Electron.*, vol. 60, no. 3, pp. 1156–1167, Mar. 2013.
[22] X. Weidong and W. G. Dunford, "A modified adaptive hill climbing MPPT method for photovoltaic power systems," in *Proc. IEEE 35th Annu. Power Electron. Spec. Conf.*, 2004, vol. 3, pp. 1957–1963.
[23] C. Huang-Jen *et al.*, "A modular self-controlled photovoltaic charger with interintegrated circuit (I^2C) interface," *IEEE Trans. Energy Convers.*, vol. 26, no. 1, pp. 281–289, Feb. 2011.
[24] N. Fermia, D. Granozio, G. Petrone, and M. Vitelli, "Predictive & adaptive MPPT perturb and observe method," *IEEE Trans. Aerosp. Electron. Syst.*, vol. 43, no. 3, pp. 934–950, Nov. 2007.
[25] N. Femia, G. Petrone, G. Spagnuolo, and M. Vitelli, "Optimization of perturb and observe maximum power point tracking method," *IEEE Trans. Power Electron.*, vol. 20, no. 4, pp. 963–973, Jul. 2005.
[26] A. K. Abdelsalam, A. M. Massoud, S. Ahmed, and P. N. Enjeti, "High-performance adaptive perturb and observe MPPT technique for photovoltaic-based microgrids," *IEEE Trans. Power Electron.*, vol. 26, no. 4, pp. 1010–1021, Jun. 2011.
[27] A. Safari and S. Mekhilef, "Simulation and hardware implementation of incremental conductance MPPT with direct control method using CUK converter," *IEEE Trans. Ind. Electron.*, vol. 58, no. 4, pp. 1154–1161, Mar. 2011.
[28] X. Weidong, W. G. Dunford, P. R. Palmer, and A. Capel, "Application of centered differentiation and steepest descent to maximum power point tracking," *IEEE Trans. Ind. Electron.*, vol. 54, no. 5, pp. 2539–2549, Aug. 2007.
[29] L. Fangrui, D. Shanxu, L. Fei, L. Bangyin, and K. Yong, "A variable step size INC MPPT method for PV systems," *IEEE Trans. Ind. Electron.*, vol. 55, no. 7, pp. 2622–2628, Jun. 2008.
[30] Y. Zhou, F. Liu, J. Yin, and S. Duan, "Study on realizing MPPT by improved incremental conductance method with variable step-size," in *Proc. 3rd IEEE Conf. Ind. Electron. Appl.*, 2008, pp. 547–550.
[31] M. Sokolov and D. Shmilovitz, "Load line emulation based maximum power point tracking," in *Proc. Power Electron. Spec. Conf.*, 2008, pp. 4098–4101.
[32] M. Sokolov and D. Shmilovitz, "A modified MPPT scheme for accelerated convergence," *IEEE Trans. Energy Convers.*, vol. 23, no. 4, pp. 1105–1107, Dec. 2008.
[33] S. Patel and W. Shireen, "Fast converging digital MPPT control for photovoltaic (PV) applications," in *Proc. Power Energy Soc. Gen. Meeting*, 2011, pp. 1–6.
[34] A. Chatterjee, A. Keyhani, and D. Kapoor, "Identification of photovoltaic source models," *IEEE Trans. Energy Convers.*, vol. 26, no. 3, pp. 883–889, Aug. 2011.
[35] K. Ishaque, Z. Salam, and S. Syafaruddin, "A comprehensive MATLAB Simulink PV system simulator with partial shading capability based on two-diode model," *Solar Energy*, vol. 85, pp. 2217–2227, 2011.
[36] F. M. Gonzalez-Longatt, "Model of photovoltaic module in MATLAB," in *Proc. 2do Congreso Iberoamericano de Estudiantes de Ingenieria Electrica, Electronica y Computacion (II CIBELEC)*, 2005, pp. 1–5.
[37] M. E. Ropp and S. Gonzalez, "Development of a MATLAB/Simulink model of a single-phase grid-connected photovoltaic system," *IEEE Trans. Energy Convers.*, vol. 24, no. 1, pp. 195–202, Feb. 2009.
[38] I. Raffaele, M. Salvatore, R. Stefano, and S. Giovanni, "An integrated approach to the simulation/optimization of grid-connected photovoltaic systems: The rational choice of components," *Int. Rev. Elect. Eng.*, vol. 7, no. 3, pp. 4596–4606, 2012.

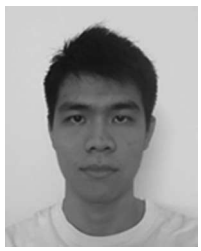

Tey Kok Soon received the B.Eng. (Hons.) and Ph.D. degrees in electrical engineering from the University of Malaya, Kuala Lumpur, Malaysia, in 2011 and 2014, respectively.

Since 2011, he has been a Research Assistant with the Power Electronics and Renewable Energy Research Laboratory (PEARL), Department of Electrical Engineering, University of Malaya. His research interests include control of converters for solar energy, power efficiency of photovoltaic (PV) system, and inverter control of PV system.

Saad Mekhilef (M'01–SM'12) received the B.Eng. degree in electrical engineering from the University of Setif, Setif, Algeria, in 1995, and the Master's degree in engineering science and Ph.D. degree in electrical engineering from the University of Malaya, Kuala Lumpur, Malaysia, in 1998 and 2003, respectively.

He is currently a Professor and Director of the Power Electronics and Renewable Energy Research Laboratory (PEARL), Department of Electrical Engineering, University of Malaya. He is the author or coauthor of more than 200 publications in international journals and proceedings. He is actively involved in industrial consultancy for major corporations in the power electronics projects. His research interests include power conversion techniques, control of power converters, renewable energy, and energy efficiency.